YMTHE, Volume *34*

Supplemental Information

Bispecific BAFF-R/BCMA CAR T cells control growth of heterogeneous plasma cells in multiple myeloma

Agnese Fiori, Karin Zimmermann, Anna Li, Jörg Westermann, Ioannis Anagnostopoulos, Lutz Menzel, Mario Bunse, Henry Erdlei, Jeyan Jayarajan, Florian Grünschläger, Juan Pablo Ortiz-Aguirre, Simon Haas, Uwe-Jens Teßmann, Jens Freitag, Andreas Rosenwald, Larry Kwak, Xiuli Wang, Zhenyuan Dong, Soungchul Cha, John Reiser, Eigen Peralta, Bahram Valamehr, Jan Krönke, Uta E. Höpken, and Armin Rehm

Supplemental Material and methods

Construction of bispecific bicistronic chimeric antigen receptors

Three bicistronic vectors encoding an anti-BAFF-R CAR and an anti-BCMA CAR linked by a P2A element were constructed using codon-optimized, synthesized DNA fragments. The first construct, "anti-BAFF-R-CD8α-28ζ 1XX-P2A-anti-BCMA-IgG1mut-28ζ 1XX" (Bi-8a-1XXz-CAR), encodes both CARs with the -1XX version of the CD3ζ activation domain. The anti-BAFF-R CAR features a CD8α hinge, spacer, and TM domain. The second construct, "anti-BAFF-R-CD8α-BBζ WT-P2A-anti-BCMA-IgG1mut-28ζ 1XX" (Bi-8a-1Bz-CAR), was derived from the first construct by replacing the intracellular signaling domains of the anti-BAFF-R CAR with the 4-1BB costimulatory domain and the unmodified CD3ζ activation domain. The third construct, "anti-BAFF-R-CD28-BBζ WT-P2A-anti-BCMA-IgG1mut-28ζ 1XX" (Bi-28-1BBz-CAR), was generated by substituting the CD8α spacer and TM domains with CD28 spacer and TM domains in the anti-BAFF-R CAR. Gene synthesis all performed by GeneArt (Thermo Fisher).

Table S1. Frequency distribution of BAFF-R expression in MM bone marrow specimen

BAFF-R expression in $CD138^+$ cells was evaluated on BM biopsies and extramedullary manifestations from 58 MM cases using immunohistochemistry. Specimens are classified as newly diagnosed MM (NDMM), post-treatment and extramedullary. Number of BAFF-R^+ and BAFF-R^- specimens are reported.

Clinical cases	**n=58**	**BAFF-R^-**	**BAFF-R^+**
NDMM	**n=20**	**9**	**11**
Post-treatment	**n=30**	**17**	**13**
Extra-medullary	**n=8**	**8**	**0**

Table S2. Antibody staining panel for the detection of plasma cells and B cells

Antibody	Fluorochrome	Clone	Isotype
BCMA (CD269)	BV421	19F2	mouse IgG2a, k
CD19	BV510	HIB19	mouse IgG1, k
CD38	FITC	HIT2	mouse IgG1, k
BAFF-R (CD268)	PE	11C1	mouse IgG1, k
CD56	PE-Cy7	5.1H11	mouse IgG1, k
CD138	APC	DL-101	mouse IgG1, k
CD3	APC-Cy7	HIT3a	mouse IgG2a, k

Table S3. Antibody panel for the detection and discrimination of CAR T cells and target cells

Antibody	Fluorochrome	Clone	Isotype
CD19	BV510	HIB19	mouse IgG1, k
CD38	FITC	HIT2	mouse IgG1, k
CD56	PE-Cy7	5.1H11	mouse IgG1, k
CD138	APC	DL-101	mouse IgG1, k
CD3	APC-Cy7	HIT3a	mouse IgG2a, k
	7-AAD		
	eFluor670		

Table S4. Antibody panel for the analysis of T cells and MM.1s tumor cells *in vivo*

T cell panel			
Antibody	**Fluorochrome**	**Clone**	**Isotype**
PD-1	PE	EH12.2H7	mouse IgG1, k
LAG-3	AF647	11C3C65	mouse IgG1, k
TIM-3	BV421	F38-2E2	mouse IgG1, k
CD8	PE-Cy7	HIT8a	mouse IgG1, k
CD3	APC-Cy7	HIT3a	mouse IgG2a, k
CAR T cell panel			
Antibody	**Fluorochrome**	**Clone**	**Isotype**
CD8	PE-Cy7	HIT8a	mouse IgG1, k
CD3	APC-Cy7	HIT3a	mouse IgG2a, k
Goat anti human IgG	PE	Polyclonal	FMO
Tumor cell panel			
Antibody	**Fluorochrome**	**Clone**	**Isotype**
CD138	BV421/APC	DL-101	mouse IgG1, k
BCMA (first antibody, unlabeled)		J22.9-FSY, human recombinant	
BAFF-R	PE/APC	11C1	mouse IgG1, k
Goat anti-human IgG (secondary antibody)	PE	Polyclonal	

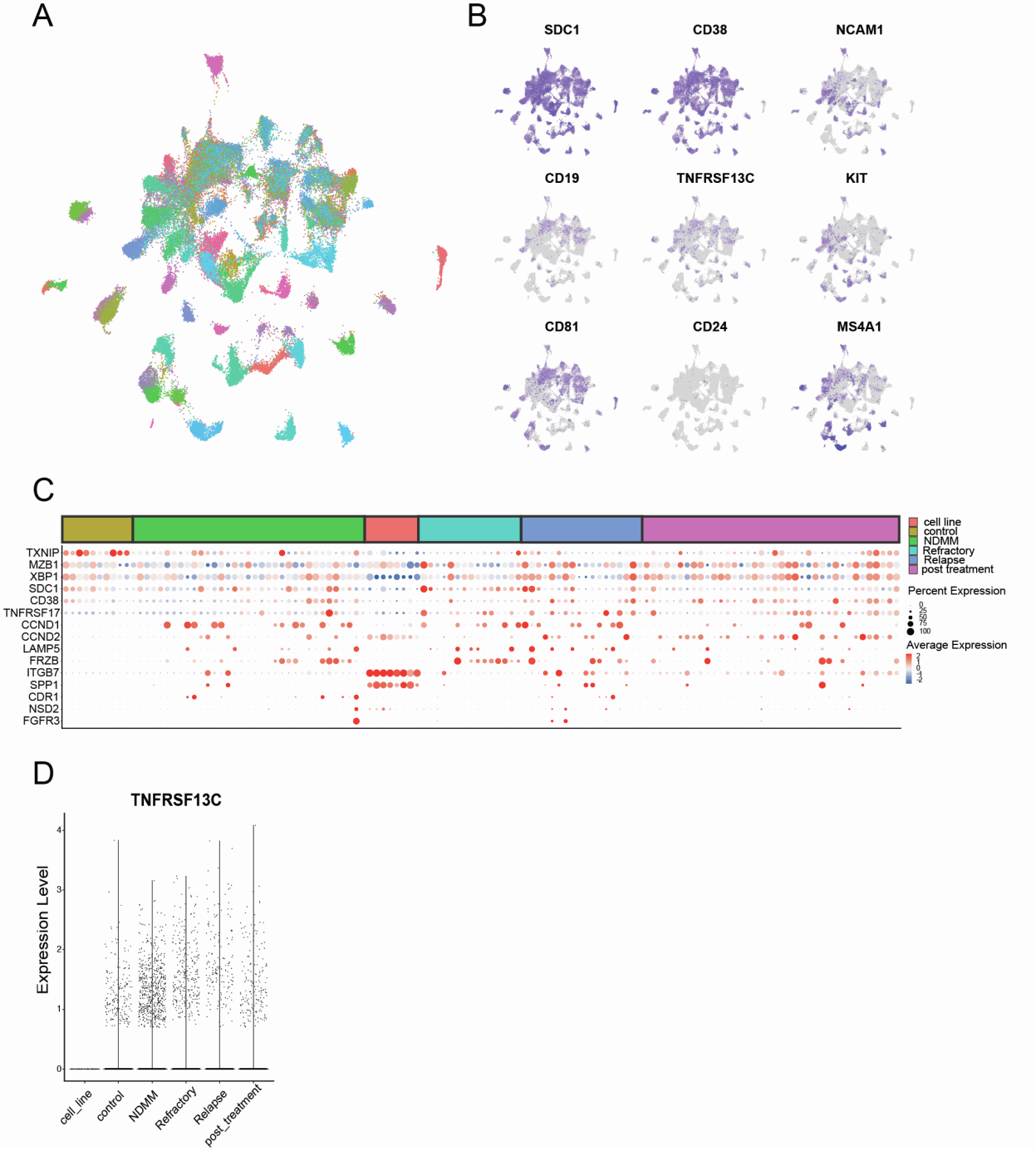

Figure S1. scRNAseq reveals the heterogeneity of Multiple Myeloma (MM) and the proportion of *TNFRSF13C*-positive malignant plasma cells in disease stages

A) UMAP plot of primary MM patient samples, showing a high heterogeneity among patients, while patients before and after treatment cluster together.

B) UMAP visualization of expression distribution of MM-associated genes in all primary MM patients. *TNFRSF13C* gene expression compared to hematopoietic stem cell markers and other MM-associated genes.
C) Enrichment of MM-signature genes in disease subgroups. MM cell lines exhibit a distinctive expression profile. Dot plot representing the size-coded percentage of MM cases expressing selected MM signature genes. Expression changes are depicted according to the color scale.
D) *TNFRSF13C* (BAFF-R) is not expressed in MM cell lines, but in primary tumor cells from all disease stages.

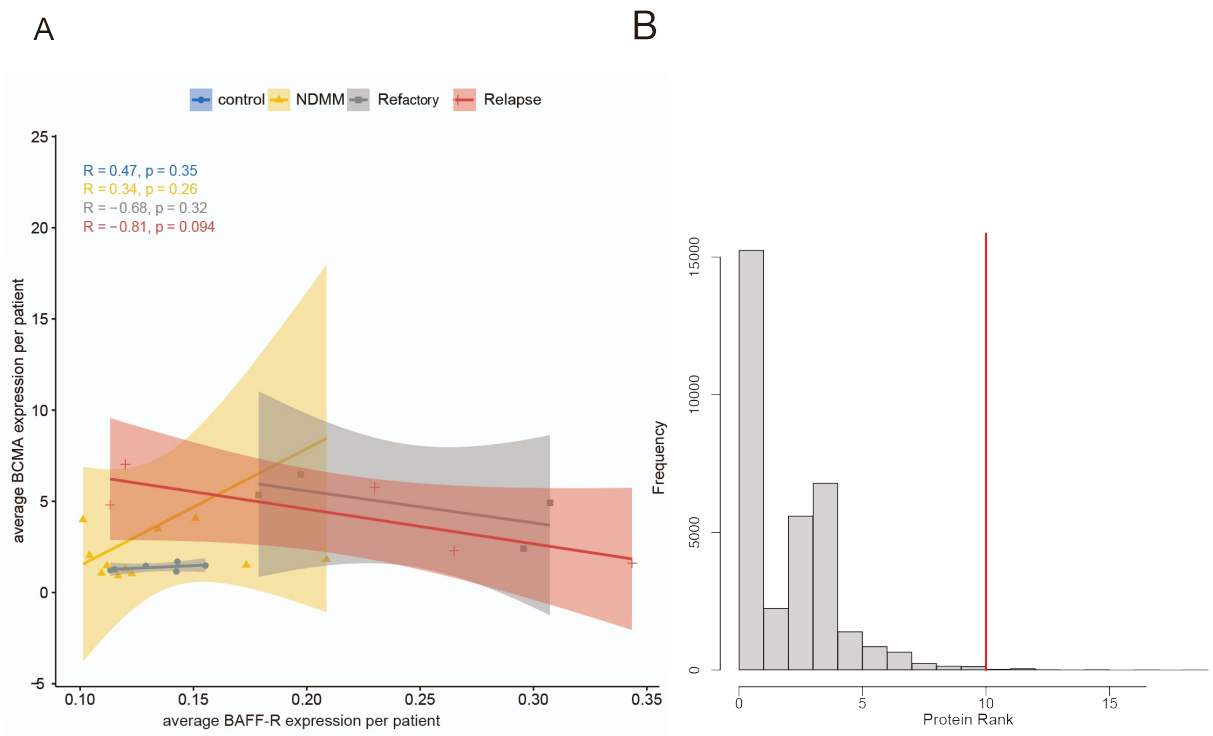

Figure S2. Correlation analysis of BCMA and BAFF-R expression in Multiple Myeloma patients

A) Correlation analysis of scRNAseq data, as in **Figure 1**. In cases of increased BAFF-R (*TNFRSF13C*) expression, control and NDMM patients show a positive correlation between BAFF-R and BCMA (*TNFRSF17*). In R/R patients, BCMA negatively correlates with an increasing BAFF-R expression.

B) Analysis of surfaceome data from Reference 43. In a ranking of potential Multiple Myeloma target antigens, BAFF-R is found in the top 1% by a combined evaluation based on gene expression and protein data. The red line indicates the rank of BAFF-R.

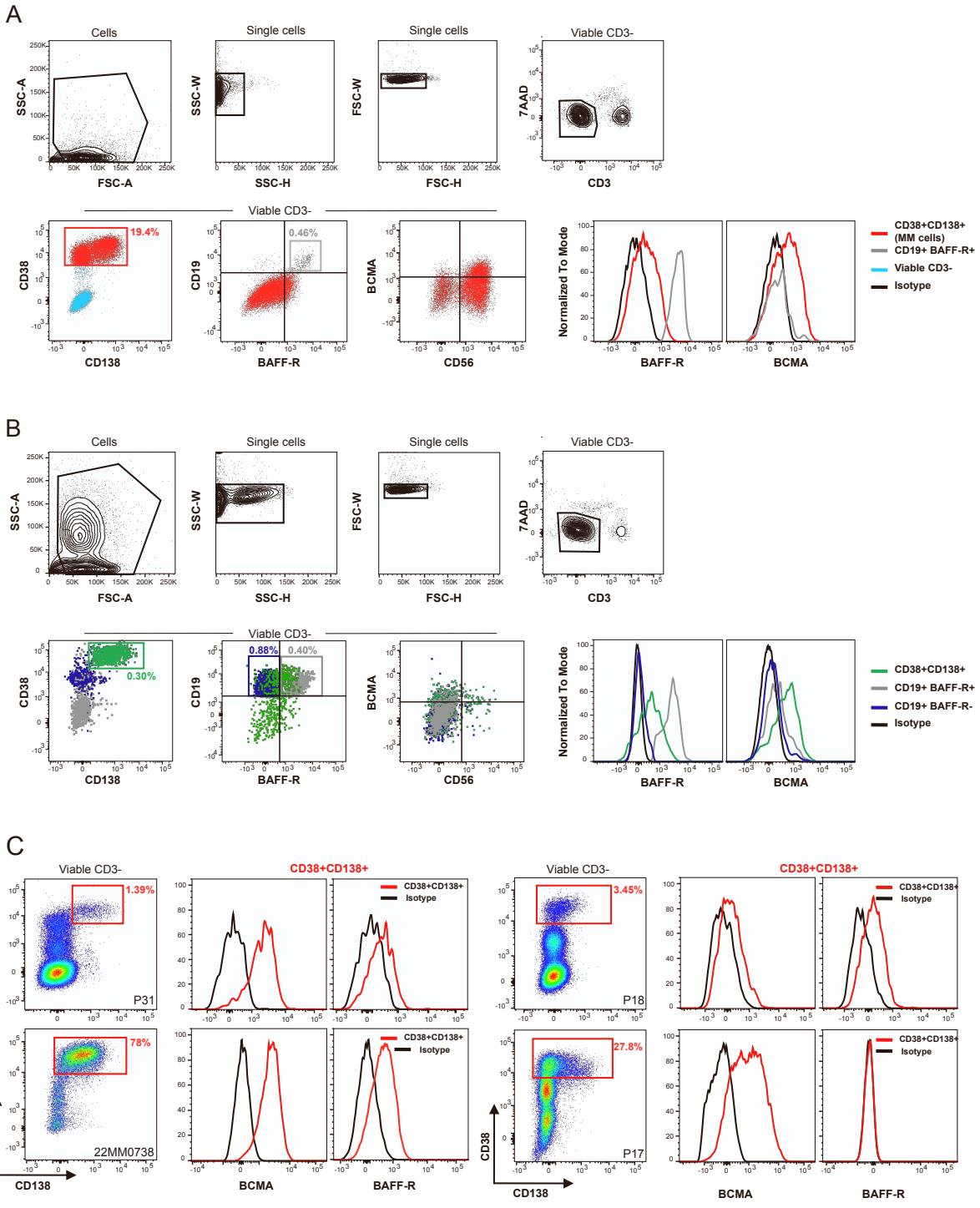
A
Cells
Single cells
Single cells
Viable CD3-
SSC-A
FSC-A
SSC-W
SSC-H
FSC-W
FSC-H
7AAD
CD3
Viable CD3-
19.4%
0.46%
CD38
CD138
CD19
BAFF-R
BCMA
CD56
Normalized To Mode
BAFF-R
BCMA
CD38+CD138+ (MM cells)
CD19+ BAFF-R+
Viable CD3-
Isotype
B
Cells
Single cells
Single cells
Viable CD3-
SSC-A
FSC-A
SSC-W
SSC-H
FSC-W
FSC-H
7AAD
CD3
Viable CD3-
0.30%
0.88%
0.40%
CD38
CD138
CD19
BAFF-R
BCMA
CD56
Normalized To Mode
BAFF-R
BCMA
CD38+CD138+
CD19+ BAFF-R+
CD19+ BAFF-R-
Isotype
C
Viable CD3-
CD38+CD138+
Viable CD3-
CD38+CD138+
1.39%
P31
CD38+CD138+
Isotype
3.45%
P18
CD38+CD138+
Isotype
78%
22MM0738
CD38+CD138+
Isotype
27.8%
P17
CD38+CD138+
Isotype
CD38
CD138
BCMA
BAFF-R
CD38
CD138
BCMA
BAFF-R

Figure S3. Flow cytometry detection of BAFF-R$^+$ expression can differentiate between PCs and B cells

A) Representative gating strategy for the characterization of malignant PCs in BM-derived MM samples. The cell population was first gated for singlets and then viable CD3$^-$ cells (light blue) are selected. Frequency of the gated populations within viable CD3$^-$ cells is reported. Histograms represent BAFF-R and BCMA in color-coded defined subpopulations. Malignant PCs are identified as CD38$^+$CD138$^+$ cells (red) and BAFF-R$^+$ B cells as CD19$^+$BAFF-R$^+$ (grey), respectively. Isotype control, black open histogram.

B) Representative gating strategy for the characterization of healthy BM specimen. The cell population was first gated for singlets and then viable CD3$^-$ cells were selected. Among those the following cell populations were defined: CD38$^+$CD138$^+$ (green), CD19$^+$BAFF-R$^-$ (blue), and CD19$^+$BAFF-R$^+$ (grey). Histograms represent BCMA and BAFF-R expression in the aforementioned populations. Isotype control, black open histogram.

C) Representative gating strategy for the detection of malignant PCs within four individual BM-derived MM samples (#P31, #22MM0738, #P18 and #P17). Malignant PCs are identified as CD38$^+$CD138$^+$ cells (red boxed gate) and their frequency among the CD3$^-$ viable population is reported. Histograms represent BCMA and BAFF-R expression in the gated population. Isotype control, black open histogram.

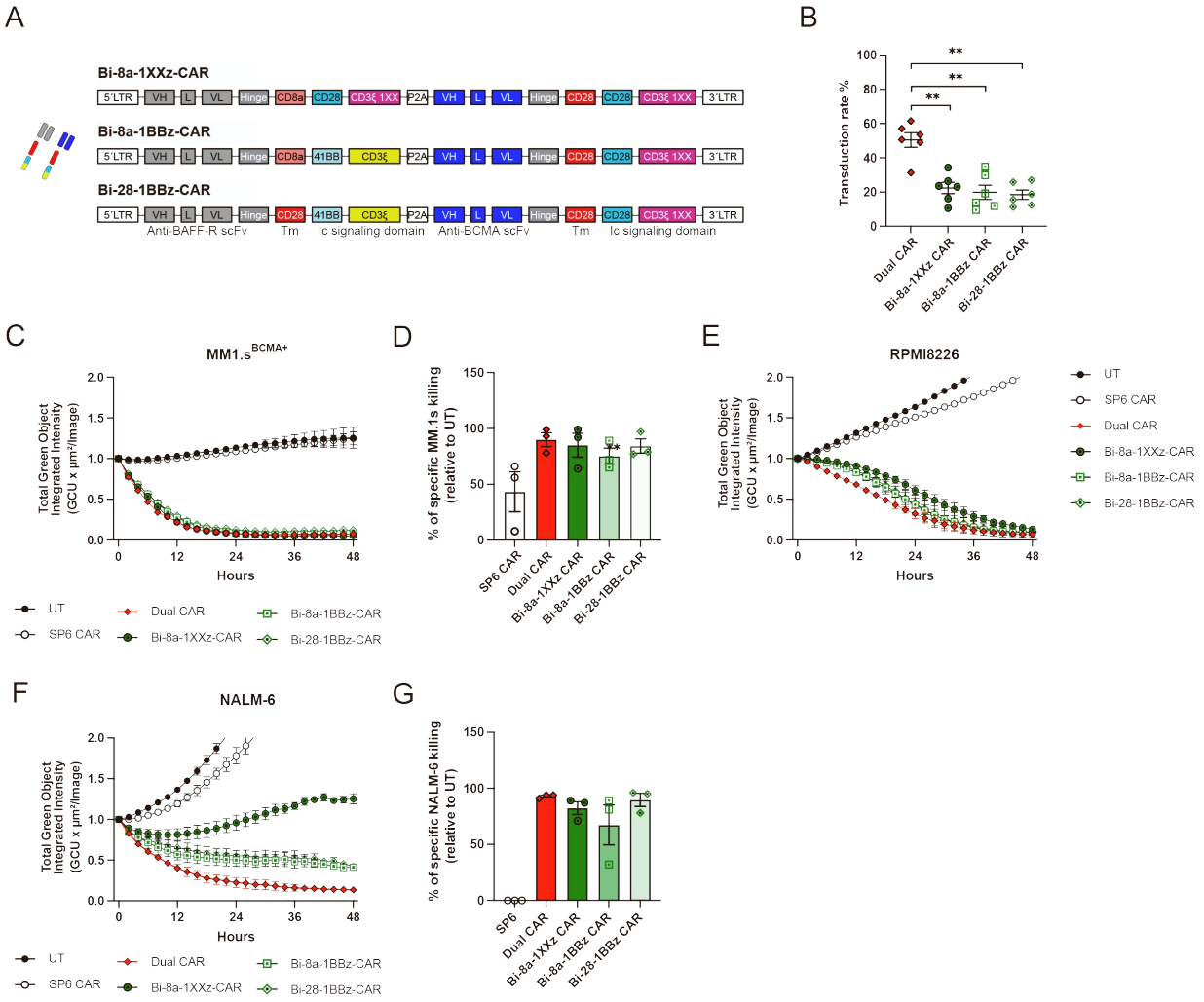

Figure S4. Bicistronic CAR designs are impaired in retroviral transduction rates, but endow T cells with efficient cytolytic capacity

A) Schematic representation of the bicistronic BAFF-R/BCMA CAR constructs Bi-8a-1XXz-CAR, Bi-8a-1BBz-CAR and Bi-28-1BBz-CAR. VH variable heavy chain, L Whitlow linker, VL variable light chain, Tm transmembrane region, Ic intracellular signalling domain, LTR long terminal repeat, Hinge human IgG1 Ch2CH3 constant region, P2A element.

B) Transduction rates in percent of T cells, data are mean ± SEM, n= 6 independent T cell donors transduced with retroviruses encoding: dual CAR, Bi-8a-1XXz-CAR, Bi-8a-1BBz-CAR and Bi-28-1BBz-CAR.

C) IncuCyte assay displaying killing kinetic of dual and bicistronic CAR T cells in coculture with GFP^+ $MM1.s^{BCMA+}$. Data are mean values ± SEM. UT n=3, SP6 CAR n=3; Dual CAR of n=2, Bi-8a-1XXz-CAR n=1, Bi-8a-1BBz-CAR n=2 and Bi-28-1BBz-CAR n=2 CAR T cell donors.

D) Flow cytometry-based cytotoxicity assay of CAR T cells and $MM.1s^{BCMA+}$ in a 1:1 E:T coculture. Specific $MM.1s^{BCMA+}$ cell killing is reported in percentage and it is calculated relative to coculture with untransduced (UT) T cells; n=3 CAR T cell donors. Mean ± SEM.

E) IncuCyte assay over 48 hours displaying killing kinetic of dual and bicistronic CAR T cells in coculture with GFP^+ RPMI-8226 MM cell line ($BCMA^+$ $BAFF\text{-}R^-$). Mean ± SEM. UT n=2, SP6 CAR n=2; Dual CAR of n=2, Bi-8a-1XXz-CAR n=2, Bi-8a-1BBz-CAR n=2 and Bi-28-1BBz-CAR n=2 CAR T cell donors.

F) Killing kinetic of dual and bicistronic CAR T cells in coculture with GFP^+ NALM-6 cells ($BAFF\text{-}R^+$ $BCMA^-$). Data are Mean ± SEM. UT n=2, SP6 CAR n=2; Dual CAR of n=2, Bi-8a-1XXz-CAR n=2, Bi-8a-1BBz-CAR n=2 and Bi-28-1BBz-CAR n=2 CAR T cell donors.

G) Flow cytometry-based cytotoxicity assay of CAR T cells and NALM-6 in 1:1 coculture. Specific NALM-6 cell killing is reported in percentage and it is calculated relative to coculture with untransduced (UT) T cells. Data are mean ± SEM. In **B**, **D)** and **G)**, statistical significance determined by Mann-Whitney test, data points represent single CAR T cell donors. **, $p<0.01$.

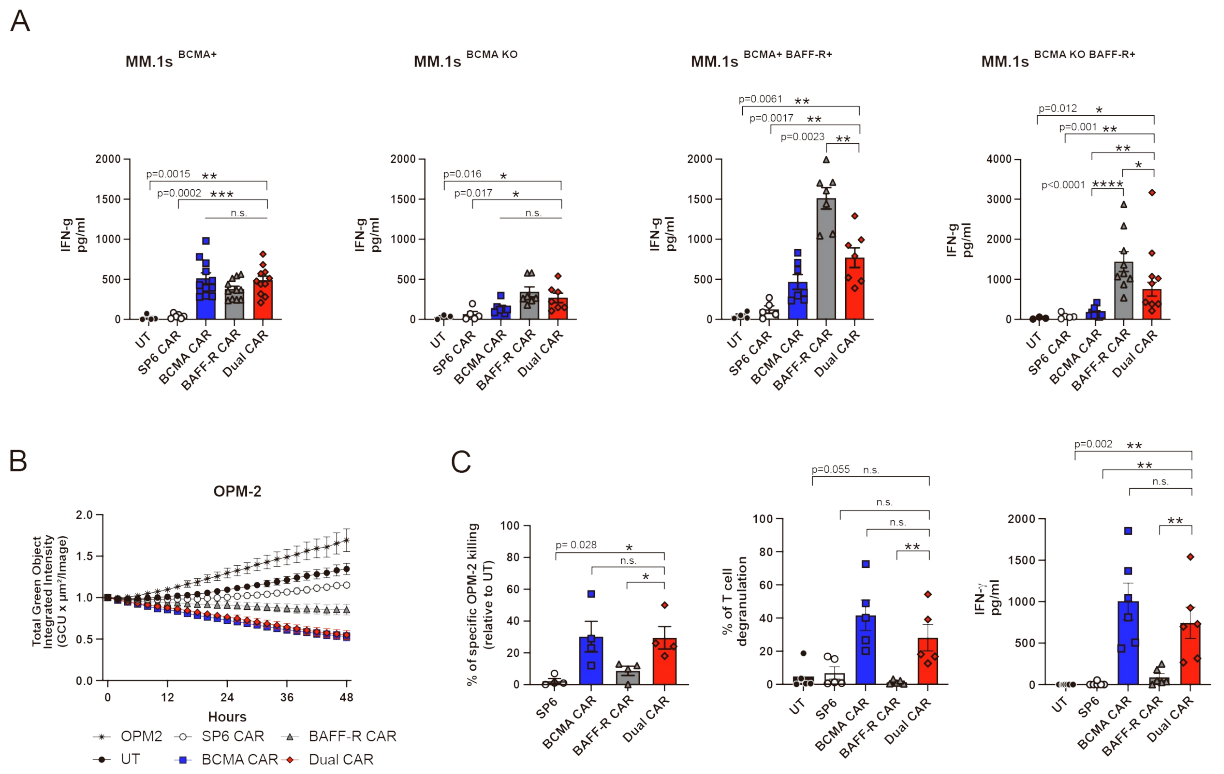

Figure S5. Dual CAR T cells exhibit similar cytolytic potency against OPM-2 MM cells as monotargeted BCMA CAR T cells

A) IFN-γ quantification in supernatants of CAR T and MM.1s cocultures after 18 hours. Mean ± SEM. Significance determined by Mann-Whitney test, data points represent single CAR T cell donors.

B) IncuCyte assay displaying killing kinetic of CAR T cells in coculture with GFP^{+} OPM-2 MM cell line (BCMA^{+} BAFF-R^{-}). Mean ± SEM. UT n=19, SP6 CAR n=19; BCMA CAR n=17, BAFF-R CAR n=17, Dual CAR of n=19 T cell donors; n=14 independent assays performed.

C) Left panel: flow cytometry-based cytotoxicity assay of CAR T cells and OPM-2 in 1:1 coculture. Specific OPM-2 cell killing is reported in percentage and it is calculated relative to coculture with untransduced (UT) T cells. Data are Mean ± SEM. Middle: percentage of CAR T cell degranulation after 4 hours of coculture with OPM-2. Mean ± SEM. Right: IFN-γ quantification in supernatants of CAR T and OPM-2 coculture after 18 hours. Mean ± SEM, a Mann-Whitney test was applied, data points represent single CAR T cell donors. n.s., non significant.

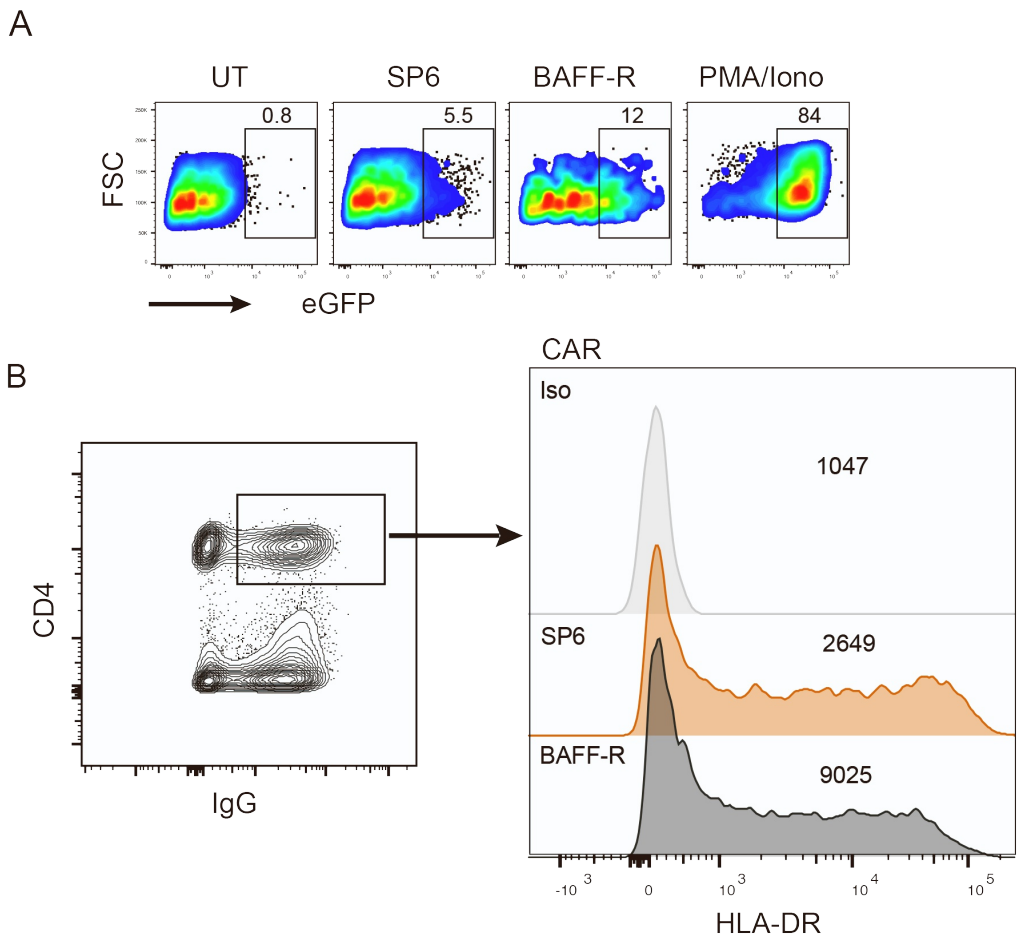

Figure S6. CAR-induced activation of an NF-KB reporter gene in Jurkat cells

A) NF-KB -eGFP Jurkat reporter cells were transduced with the CAR constructs as indicated; UT, untransduced. Ten days after retroviral transduction, CAR^+ Jurkat cells were analyzed for GFP expression by FACS; PMA/ionomycin used as a positive control for activation. Numbers on the gates indicate the frequency in percent of GFP-positive reporter cells. n=2 independent experiments.

B) Primary human T cells were transduced with the CAR constructs as indicated. At day ten, CAR^+ $CD4^+$ T cells were analyzed for HLA-DR (LN3 antibody) expression; gMFI values are given in the histograms. Iso, isotype control. n=2 independent experiments.

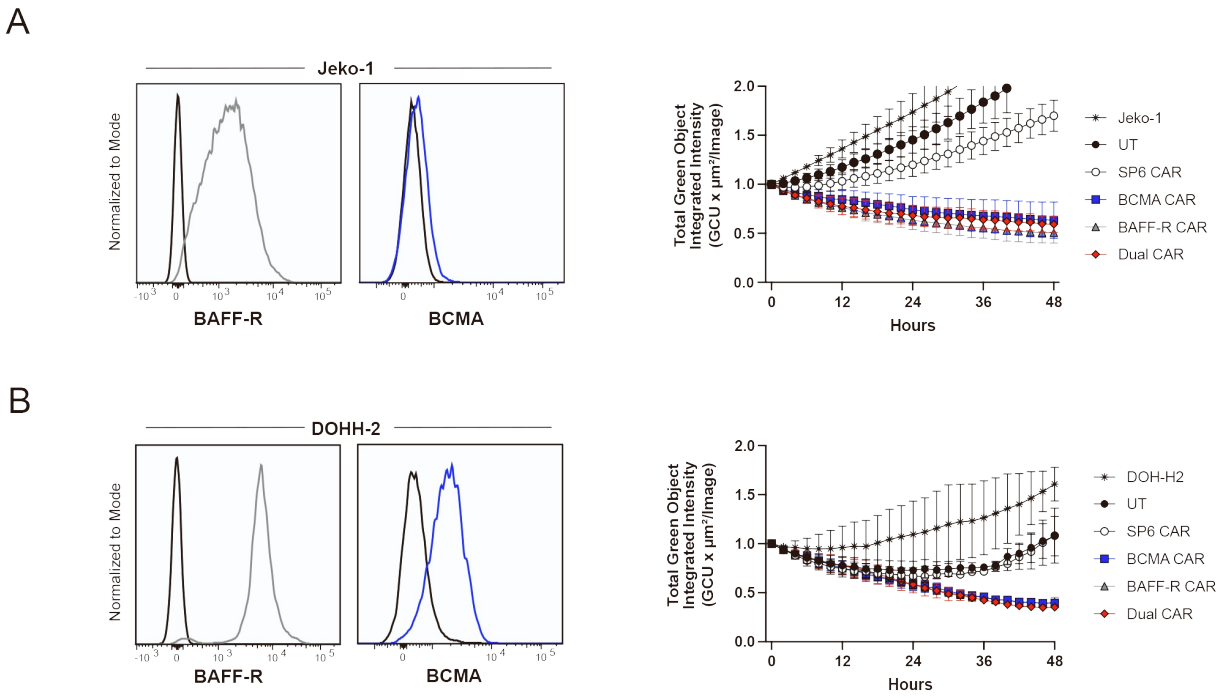

Figure S7. BCMA^{low} expressing B-NHL cell lines are efficiently targeted by dual CAR T cells

A) Flow cytometry analysis of JeKo-1 mantle cell lymphoma cell line stained with anti-BAFF-R and anti-BCMA antibodies. Isotype control, black line; blue line, BCMA expression. On the right, IncuCyte assay for CAR T cells in coculture with GFP$^+$ Jeko-1 B-NHL cell line (BCMA$^+$ BAFF-R$^+$). Mean ± SEM. UT n=7, SP6 CAR n=7; BCMA CAR n=7, BAFF-R CAR n=7, Dual CAR of n=7 T cell donors; n=2 independent experiments performed.

B) On the left, FACS histograms of antibody stained DOHH-2 cell line (immunoblastic lymphoma, DLBCL). Right: IncuCyte assay for CAR T cells in coculture with GFP$^+$ DOHH-2 cell line (BCMA$^+$ BAFF-R$^+$). Mean ± SEM. UT n=4, SP6 CAR n=4; BCMA CAR n=4 BAFF-R CAR n=4, Dual CAR of n=4 T cell donors; DOHH-2 n=2.

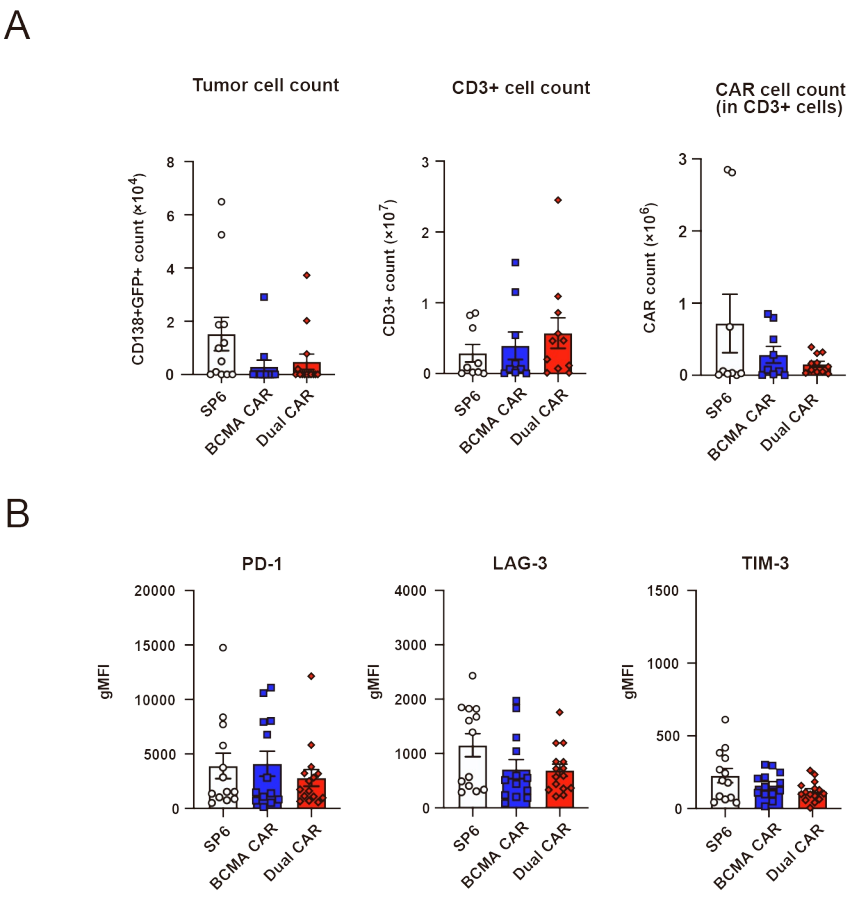

Figure S8. Efficient and comparable depletion of MM.1s tumor cell count in spleen of BCMA CAR and dual CAR T cell treated NSG mice

A) Counts of tumor cells ($CD138^{+}GFP^{+}$ cells), $CD3^{+}$ T cells and CAR T cells in spleen.

B) gMFI of PD-1, LAG-3 and TIM-3 exhaustion markers in CD3 cells in spleen. In **A)** and **B)**, mean values ± SEM, n= 3 independent experiments, data points represent individual animals.

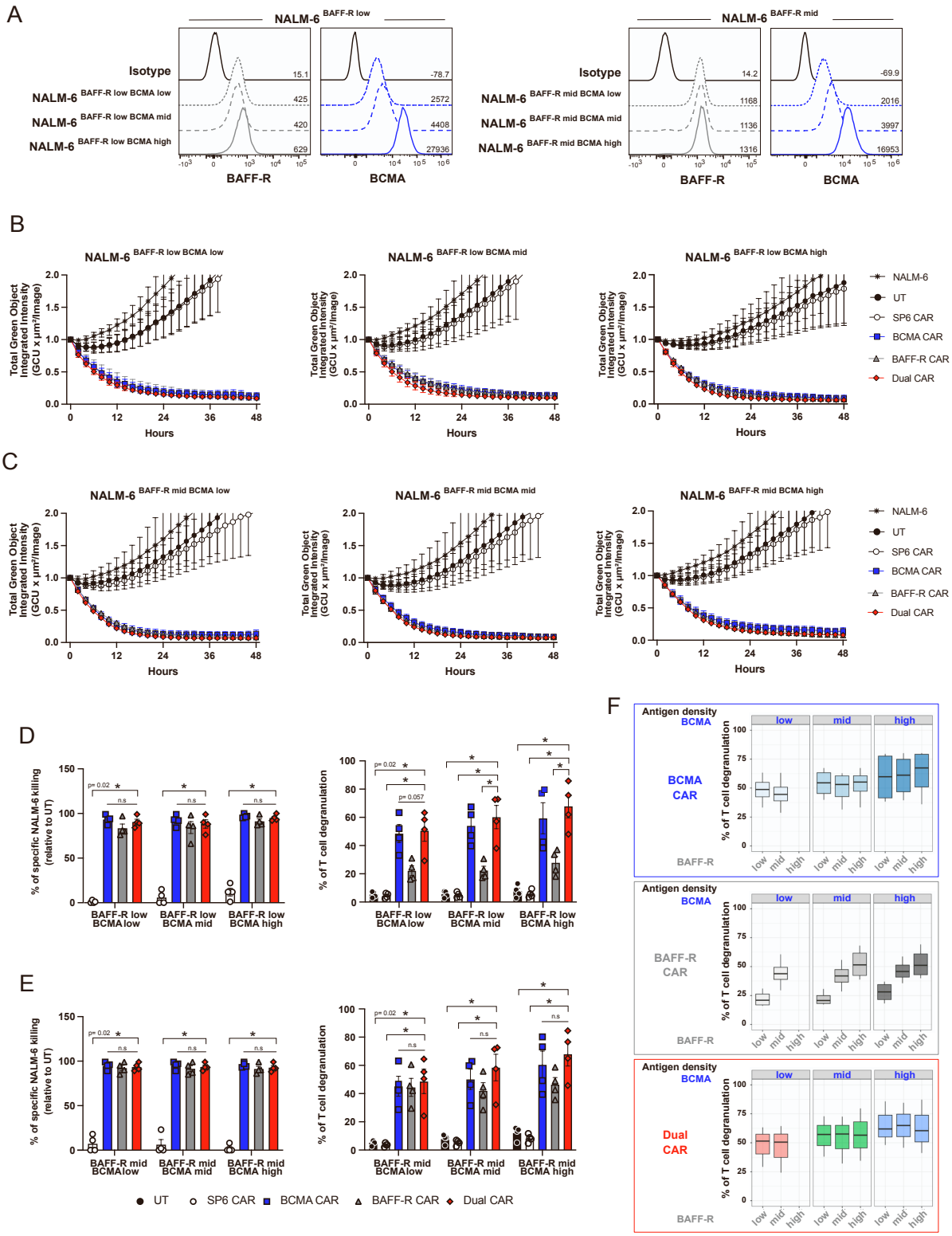
A
NALM-6 BAFF-R low
NALM-6 BAFF-R mid
Isotype
NALM-6 BAFF-R low BCMA low
NALM-6 BAFF-R low BCMA mid
NALM-6 BAFF-R low BCMA high
NALM-6 BAFF-R mid BCMA low
NALM-6 BAFF-R mid BCMA mid
NALM-6 BAFF-R mid BCMA high
BAFF-R
BCMA
B
C
Total Green Object Integrated Intensity (GCU x µm²/Image)
Hours
NALM-6
UT
SP6 CAR
BCMA CAR
BAFF-R CAR
Dual CAR
D
E
% of specific NALM-6 killing (relative to UT)
% of T cell degranulation
F
Antigen density
BCMA
BAFF-R
low
mid
high
BCMA CAR
BAFF-R CAR
Dual CAR

Figure S9. Antigen specificity of dual CAR T cells

A) BAFF-R (grey) and BCMA (blue) antigen expression on NALM-6 cells with titrated amounts of BAFF-R and BCMA. NALM-6 cells were first silenced for BAFF-R expression, and then sequentially transduced for BAFF-R and BCMA. Cells with distinct expression levels were sorted by flow cytometry. For BCMA detection, antibody clone 19F2 was used. gMFI values for the tested antigen are reported. Isotype controls: black open histogram. Representative plots.

B) and **C)** IncuCyte assays of CAR T cells in coculture with GFP^+ NALM-6 cells with various expression levels low-mid-high for BAFF-R and BCMA, as indicated. Mean ± SEM. UT, SP6 CAR, BCMA CAR, BAFF-R CAR, Dual CAR n=5 T cell donors; n=7 independent experiments performed.

D) and **E)** Left panels: FACS-based cytotoxicity assay of CAR T cells and NALM-6 with various BAFF-R and BCMA expression levels in a 1:1 coculture. NALM-6 cell killing is reported in percentage, calculated relative to UT T cells.

Middle: percentage of CAR T cell degranulation after 4 hours of coculture with NALM-6.

Mean ± SEM with p-value in **D)** and **E)** by Mann-Whitney test, data points represent single CAR T cell donors. *, $p<0.05$; n.s., non significant.

F) Quantification of antigen-dependent degranulation capacity of either BCMA CAR (left), BAFF-R CAR (middle), and dual CAR (right panel). On the top of each box and whisker plot, BCMA expression levels are given. On the bottom, corresponding antigen densities for BAFF-R are depicted. Regardless of BCMA antigen density, reactivity of the BAFF-R CAR correlates with increasing BAFF-R antigen expression.